Model Order Reduction for Linear Time-invariant System with Symmetric Positive Definite Matrices: Synthesis of Cauer-equivalent Circuit

Shingo Hiruma[1,2], and Hajime Igarashi[1], *IEEE Member*

[1]Graduate School of Information Science and Technology, Hokkaido University, Hokkaido 060-0814, Japan
[2]Research Fellow of Japan Society for the Promotion of Science (JSPS), Tokyo 102-0083, Japan

This paper introduces a new model order reduction method for a linear time-invariant system with symmetric positive definite matrices. The proposed method allows the construction of a reduced model, represented by a Cauer-equivalent circuit, from the original system. The method is developed by extending the Cauer ladder network method for the quasi-static Maxwell's equations, which is shown to be regarded as the Lanczos algorithm with respect to a self-adjoint matrix. As a numerical example, a Cauer-equivalent circuit is generated from a simple mathematical model as well as the finite element (FE) model of a magnetic reactor that is driven by a pulse width modulation voltage wave. The instantaneous power obtained from the circuit analysis is shown to be in good agreement with that obtained from the original FE model.

***Index Terms*—continued fraction, Krylov subspace methods, Lanczos algorithm, Padé approximation, self-adjoint matrix, transfer function**

I. Introduction

The finite element method (FEM) has been widely used for the analysis of electric machines and devices such as electric motors, inductors, and transformers. In recent years, it has become more important to evaluate the eddy current losses using FEM because the switching frequency of power electronics circuits has increased [1]. However, FE analysis is frequently extremely time-consuming to use for the optimal design of electric apparatuses for which the analysis is performed for different design parameters and different driving methods numerous times. Therefore, equivalent circuits are regularly adopted for the design of electric apparatuses as well as driving systems. However, using equivalent circuits it is difficult to know how the changes in the geometry and material property affect the machine performance. Moreover, it is also not easy to accurately evaluate the eddy current losses using this classical approach. Thus, a reduction in the computational cost of FEM is required.

An efficient approach to reduce the computational cost of FE analysis is to use the model order reduction (MOR) method, which generates a reduced model of a high-dimensional system. There have been many studies on the MOR methods that are based on the proper orthogonal decomposition (POD)[2][3][4][5] and Krylov subspace methods[6][7][8][9]. The Padé via Lanczos (PVL) approximation [6] is one of the Krylov subspace methods that reduce a given transfer function to a rational function. By applying the PVL approximation to a linear dynamical system, we can obtain from an original system a partial fraction that is equivalent to a Foster circuit, which can be conveniently analyzed by circuit simulators such as SPICE.

A limitation in applying the PVL approximation to the analysis of electric apparatuses is that it is difficult to represent a nonlinear saturation property of a magnetic core using the resulting Foster circuit. To overcome this problem, Sato and Igarashi[9][10] proposed a method in which nonlinearity was introduced in a Cauer circuit that was converted from the Foster circuit by the Euclidean algorithm. In this method, a pre-computed current-flux characteristic was embedded in the inductor in the first stage of the Cauer circuit to represent the nonlinearity due to the magnetic saturation.

Recently, Kameari et al. proposed a method to obtain a Cauer circuit from quasi-static Maxwell's equations, which was referred to as the Cauer ladder network (CLN)[11]. In contrast to the methods based on the PVL approximation, the CLN method can generate Cauer circuits directly from Maxwell's equations without the Euclidean algorithm. However, it has been difficult to apply CLN to systems that are not governed by the quasi-static Maxwell's equations. In addition, the relationship between the PVL and CLN methods has been unclear partially because the latter is formulated in a continuous system whereas the former is formulated in a discrete system.

In this paper, we show that the CLN method can be regarded as the Lanczos algorithm with respect to a self-adjoint matrix. Based on this fact and extending the CLN method, we propose a new method for model order reduction. The proposed method can be applied not only to discrete quasi-static Maxwell's equations but also to general discrete systems with a positive definite symmetric matrix.

This paper is organized as follows. In section II, we formulate the CLN method and its discrete version. We discuss the relation between the discrete version of the CLN method and Lanczos algorithm. In section III, we introduce a new method to obtain the continued fraction expansion of a given transfer function. In section IV, the proposed method is verified by applying it to a simple mathematical problem

Manuscript received December 1, 2012; revised December 27, 2012.
Corresponding author: Shingo Hiruma (email: hiruma@em.ist.hokudai.ac.jp).

as well as a magnetic reactor model. Finally, the paper is concluded in section V with a concise summary of the study and perspectives for future work.

II. CLN METHOD

The CLN method is derived under the assumption that a Cauer circuit is constructed by the expansion of the quasi-static electromagnetic field in terms of orthogonal functions. This assumption is based on the analysis of a one-dimensional (1D) magnetic steel sheet. The quasi-static electromagnetic field in a magnetic steel sheet can be represented by the linear combination of Legendre polynomials. It is known that the norms of Legendre polynomials correspond to the circuit parameters in a Cauer circuit[12]. In addition, the expansion coefficients of the magnetic and electric fields correspond to the currents and voltages in a Cauer circuit, respectively. Thus, the coefficients satisfy the Kirchhoff voltage law (KVL) and Kirchhoff current law (KCL). Kameari et al. developed the CLN method assuming that this fact holds also in three-dimensional (3D) quasi-static Maxwell's equations.

In this section, after we provide a summary of the CLN method, we formulate the discrete version of the CLN method, which makes it easier to consider the relation with the Lanczos algorithm.

A. introduction of CLN method

Let Ω be the analysis domain bounded by $\Gamma = \partial\Omega$, as shown in Fig.1. Boundary Γ includes Γ_{in} and Γ_{out} through which the external current flows into and out of the domain, respectively. We consider the electromagnetic fields in Ω to be governed by quasi-static Maxwell's equations

$$\nabla \times \boldsymbol{H}(t,\boldsymbol{x}) = \sigma \boldsymbol{E}(t,\boldsymbol{x}), \tag{1a}$$

$$\nabla \times \boldsymbol{E}(t,\boldsymbol{x}) = -\frac{\partial \boldsymbol{B}(t,\boldsymbol{x})}{\partial t} \tag{1b}$$

where $\boldsymbol{H}(t,\boldsymbol{x})$, $\boldsymbol{B}(t,\boldsymbol{x})$, $\boldsymbol{E}(t,\boldsymbol{x})$, and σ represent the magnetic field, magnetic flux density, electric field, and conductivity, respectively.

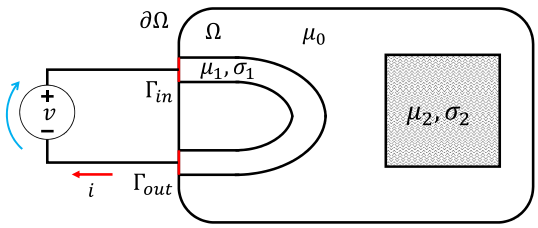

Fig. 1. Analysis domain and external power supply

To obtain a Cauer circuit as shown in Fig.2, $\boldsymbol{H}(t,\boldsymbol{x})$ and $\boldsymbol{E}(t,\boldsymbol{x})$ are supposed to be written as

$$\boldsymbol{H}(t,\boldsymbol{x}) = \sum_{n=0}^{\infty} h_n(t)\boldsymbol{H}_n(\boldsymbol{x}), \tag{2a}$$

$$\boldsymbol{E}(t,\boldsymbol{x}) = \sum_{n=0}^{\infty} e_n(t)\boldsymbol{E}_n(\boldsymbol{x}), \tag{2b}$$

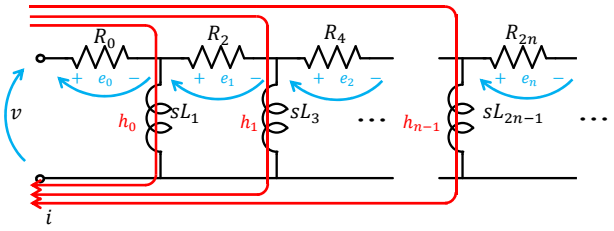

Fig. 2. Cauer circuit

where $h_n(t)$, $e_n(t)$, and $\boldsymbol{H}_n(\boldsymbol{x})$, $\boldsymbol{E}_n(\boldsymbol{x})$ are the functions of time t and position $\boldsymbol{x}$, respectively. With reference to the analysis of a 1D magnetic steel sheet, it is assumed heuristically that the coefficients satisfy KVL and KCL of the Cauer circuit, which are given by

$$-L_1\frac{dh_1}{dt} = e_0 - v, \qquad -L_{2n+1}\frac{dh_n}{dt} + L_{2n-1}\frac{dh_{n-1}}{dt} = e_n, \tag{3a}$$

$$\frac{e_0}{R_0} = i, \qquad \frac{e_n}{R_{2n}} - \frac{e_{n+1}}{R_{2n+2}} = h_{n+1}. \tag{3b}$$

Instantaneous Joule losses $P(t)$ and magnetic energy $W(t)$ are written as

$$2W(t) = (\mu\boldsymbol{H},\boldsymbol{H})_\Omega = \sum_{n=0}^{\infty} L_{2n+1}h_{2n+1}^2(t), \tag{4a}$$

$$P(t) = (\sigma\boldsymbol{E},\boldsymbol{E})_\Omega = \sum_{n=0}^{\infty} \frac{e_{2n}^2(t)}{R_{2n}} \tag{4b}$$

The inner products in (4) are defined in the analysis domain (Fig.1), and the right-hand sides are from the Cauer circuit (Fig.2). The equations (4) are required to hold the energy conservation law. From (2), (4), it is concluded that $\boldsymbol{H}_n(\boldsymbol{x})$, $\boldsymbol{E}_n(\boldsymbol{x})$ must satisfy the orthogonality:

$$(\boldsymbol{H}_m,\mu\boldsymbol{H}_n)_\Omega = \int_\Omega \boldsymbol{H}_m\cdot\mu\boldsymbol{H}_n d\Omega = L_{2n+1}\delta_{mn}, \tag{5a}$$

$$(\boldsymbol{E}_m,\sigma\boldsymbol{E}_n)_\Omega = \int_\Omega \boldsymbol{E}_m\cdot\sigma\boldsymbol{E}_n d\Omega = \frac{1}{R_{2n}}\delta_{mn}, \tag{5b}$$

where μ denotes the permeability and δ_{mn} denotes the Kronecker delta. The orthogonal functions can be constructed by the Gram–Schmidt orthogonalization. They can also be determined from the two-term recursion relation derived from (1) and (3). Thus, substituting (2) into (1) and considering (3), we obtain

$$\nabla\times(\boldsymbol{H}_{n+1}-\boldsymbol{H}_n) = \nabla\times\tilde{\boldsymbol{H}}_{n+1} = R_{2n}\sigma\boldsymbol{E}_n \tag{6a}$$

$$\nabla\times(\boldsymbol{E}_n-\boldsymbol{E}_{n-1}) = \nabla\times\tilde{\boldsymbol{E}}_n = -\frac{1}{L_{2n-1}}\mu\boldsymbol{H}_{n-1} \tag{6b}$$

where $\boldsymbol{E}_{-1} = \boldsymbol{0}$, $\boldsymbol{H}_{-1} = \boldsymbol{0}$. We can obtain the orthogonal functions by iteratively solving the two-term recursion relation. The algorithm of the CLN is summarized in Algorithm 1. Note that the equations in the algorithm are solved under appropriate boundary conditions.

Algorithm 1 Framework of the CLN

1: Find electric field $\boldsymbol{E}_0$ that satisfies $\nabla \times \boldsymbol{E}_0 = 0$ with 1 V of power supply .
2: Compute R_0 by (5).
3: **for** n=1 to q **do**
4: Solve $\nabla \times \tilde{\boldsymbol{H}}_n = R_{2n-2}\sigma \boldsymbol{E}_{n-1}$
5: Set $\boldsymbol{H}_n = \boldsymbol{H}_{n-1} + \tilde{\boldsymbol{H}}_n$
6: Compute L_{2n-1} by (5).
7: Solve $\nabla \times \tilde{\boldsymbol{E}}_n = -\frac{1}{L_{2n-1}}\mu \boldsymbol{H}_n$
8: Set $\boldsymbol{E}_n = \boldsymbol{E}_{n-1} + \tilde{\boldsymbol{E}}_n$
9: Compute R_{2n} by (5).
10: **end for**

B. Discrete CLN method

In this subsection, we derive the discrete CLN method by applying FE discretization to (1). Analysis domain Ω is subdivided into FEs. The vector potential and electric field are discretized as

$$\boldsymbol{A} = \sum_{i=1}^{n_e} a_i \boldsymbol{N}_i, \tag{7a}$$

$$\boldsymbol{E} = \sum_{i=1}^{n_e} e_i \boldsymbol{N}_i \tag{7b}$$

where n_e is the number of the edges, $\boldsymbol{a} = [a_1\ a_2\ \cdots\ a_{n_e}]^{\mathrm{T}} \in \mathbb{R}^{n_e}$, and $\boldsymbol{e} = [e_1\ e_2\ \cdots\ e_{n_e}]^{\mathrm{T}} \in \mathbb{R}^{n_e}$. Inserting (7) in (5) results in

$$(\boldsymbol{H}_m, \mu \boldsymbol{H}_n)_\Omega = \boldsymbol{a}_m^{\mathrm{T}} \mathrm{K} \boldsymbol{a}_n = (\boldsymbol{a}_m, \boldsymbol{a}_n)_{\mathrm{K}} = L_{2n+1}\delta_{mn}, \tag{8a}$$

$$(\boldsymbol{E}_m, \sigma \boldsymbol{E}_n)_\Omega = \boldsymbol{e}_m^{\mathrm{T}} \mathrm{N} \boldsymbol{e}_n = (\boldsymbol{e}_m, \boldsymbol{e}_n)_{\mathrm{N}} = \frac{1}{R_{2n}}\delta_{mn} \tag{8b}$$

where $\boldsymbol{H}_n = \frac{1}{\mu}\mathrm{rot}\boldsymbol{A}_n$, $\boldsymbol{A}_n = \mathrm{N}\boldsymbol{a}_n$, $\boldsymbol{E}_n = \mathrm{N}\boldsymbol{e}_n$, and $\mathrm{K} \in \mathbb{R}^{n_e \times n_e}$, $\mathrm{N} \in \mathbb{R}^{n_e \times n_e}$ are the FE matrices Matrices K and N are symmetric positive definite matrices[1]. Brackets $(\cdot,\cdot)_{\mathrm{K}}$ and $(\cdot,\cdot)_{\mathrm{N}}$ in (8) are known as the generalizations of the inner product, referred to as the K and N inner product, respectively. All the equations in Algorithm 1 are discretized by using FEM, as shown in Algorithm 2.

Algorithm 2 Framework of the discrete CLN

1: Find the solution of discretized Laplace equation $\mathrm{G}\boldsymbol{e}_0 = \boldsymbol{b}$.
2: Compute R_0 by (8).
3: **for** n=1 to q **do**
4: Solve $\mathrm{K}\tilde{\boldsymbol{a}}_n = R_{2n-2}\mathrm{N}\boldsymbol{e}_{n-1}$
5: Set $\boldsymbol{a}_n = \tilde{\boldsymbol{a}}_n + \boldsymbol{a}_{n-1}$.
6: Compute L_{2n-1} by (8).
7: Set $\tilde{\boldsymbol{e}}_n = -\frac{1}{L_{2n-1}}\boldsymbol{a}_n$
8: Set $\boldsymbol{e}_n = \boldsymbol{e}_{n-1} + \tilde{\boldsymbol{e}}_n$.
9: Compute R_{2n} by (8).
10: **end for**

We can derive a two-term recursion relation similar to (6); the equations in steps 5 and 8 in Algorithm 2 can be written as

$$\boldsymbol{a}_n = \boldsymbol{a}_{n-1} - R_{2n-2}\mathrm{A}\boldsymbol{e}_{n-1}, \tag{9a}$$

$$\boldsymbol{e}_n = \boldsymbol{e}_{n-1} - \frac{1}{L_{2n-1}}\boldsymbol{a}_n. \tag{9b}$$

where $\mathrm{A} = -\mathrm{K}^{-1}\mathrm{N}$. We can find that vectors $\boldsymbol{a}_n$ and $\boldsymbol{e}_n$ are the orthogonal bases of the Krylov subspace, i.e.,

$$\boldsymbol{a}_n \in \mathcal{K}_n(\mathrm{A}, \boldsymbol{e}_0), \tag{10a}$$

$$\boldsymbol{e}_n \in \mathcal{K}_n(\mathrm{A}, \boldsymbol{e}_0) \tag{10b}$$

where $\mathcal{K}_n(\mathrm{A}, \boldsymbol{e}_0) = \mathrm{span}(\boldsymbol{e}_0, \mathrm{A}\boldsymbol{e}_0, \cdots, \mathrm{A}^{n-1}\boldsymbol{e}_0)$. We can derive a three-term recursion relation from (9) as follows:

$$\mathrm{A}\Big(\sum_{i=0}^{n-1} \frac{1}{L_{2i-1}}\boldsymbol{a}_i\Big) = \frac{1}{R_{2n-2}}(\boldsymbol{a}_n - \boldsymbol{a}_{n-1}). \tag{11}$$

By subtracting (11) for $n+1$ from that for n results in

$$\mathrm{A}\boldsymbol{a}_n = \frac{L_{2n-1}}{R_{2n}}\boldsymbol{a}_{n+1} - L_{2n-1}\Big(\frac{1}{R_{2n}} + \frac{1}{R_{2n-2}}\Big)\boldsymbol{a}_n + \frac{L_{2n-1}}{R_{2n-2}}\boldsymbol{a}_{n-1} \tag{12}$$

Similarly, we obtain

$$\mathrm{A}\boldsymbol{e}_n = \frac{L_{2n+1}}{R_{2n}}\boldsymbol{e}_{n+1} - \frac{1}{R_{2n}}(L_{2n+1} + L_{2n-1})\boldsymbol{e}_n + \frac{L_{2n-1}}{R_{2n}}\boldsymbol{e}_{n-1}. \tag{13}$$

C. Relation to Lanczos algorithm

In this subsection, we introduce a self-adjoint matrix and discuss its properties. Let $\mathrm{A} \in \mathbb{R}^{N\times N}$, and $\mathrm{G} \in \mathbb{R}^{N\times N}$ be a symmetric positive definite matrix. Matrix $\mathrm{A}^{\#} \in \mathbb{R}^{N\times N}$is referred to as the G adjoint matrix when the following relation holds:

$$(\boldsymbol{x}, \mathrm{A}\boldsymbol{y})_{\mathrm{G}} = (\mathrm{A}^{\#}\boldsymbol{x}, \boldsymbol{y})_{\mathrm{G}} \quad \forall\, \boldsymbol{x}, \boldsymbol{y} \in \mathbb{R}^N. \tag{14}$$

In particular, if $\mathrm{A} = \mathrm{A}^{\#}$, A is referred to as the G self-adjoint matrix. The definition of the G self-adjoint matrix is a natural extension of a symmetric matrix because A becomes symmetric if $\mathrm{G} = \mathrm{I}$, where I is a unit matrix. As is the case of a symmetric matrix, a three-term recursion relation is derived as shown in the following proposition: Let $\mathrm{G} \in \mathbb{R}^{N\times N}$ be a symmetric positive definite matrix, and $\mathrm{A} \in \mathbb{R}^{N\times N}$ be a G self-adjoint matrix. Let $\boldsymbol{u}_0 \in \mathbb{R}^N$ be an arbitrary non-zero vector. If vectors $\boldsymbol{u}_k \in \mathcal{K}_k(\mathrm{A}, \boldsymbol{u}_0)$ $(k = 0, 1, \cdots, \hat{k})$ are orthogonal with respect to the G inner product

$$(\boldsymbol{u}_i, \boldsymbol{u}_j)_{\mathrm{G}} = \kappa_i \delta_{ij}, \tag{15}$$

and $\boldsymbol{u}_k \neq \boldsymbol{0}$, there exist ζ_k, η_k, and $\xi_k \in \mathbb{R}$ that satisfy the three-term recursion

$$\mathrm{A}\boldsymbol{u}_k = \zeta_k \boldsymbol{u}_{k+1} + \eta_k \boldsymbol{u}_k + \xi_k \boldsymbol{u}_{k-1} \tag{16}$$

where $\boldsymbol{u}_0 = \boldsymbol{1}$, $\boldsymbol{u}_{-1} = \boldsymbol{0}$. This three-term recursion is a generalization of the form appearing in the Lanczos algorithm [13] [14]. The following well-known lemma help us link the discrete CLN method to the Lanczos algorithm with respect to a self-adjoint matrix. Let $\mathrm{K}, \mathrm{N} \in \mathbb{R}^{N\times N}$ be symmetric positive definite matrices and $\mathrm{A} = -\mathrm{K}^{-1}\mathrm{N}$. Then A is a K

[1]It is assumed here that the redundant unknowns are eliminated for K and the air region has a low conductivity for N. It is, however, numerically confirmed that the algorithm works well even if these assumptions are relaxed.

self-adjoint matrix as well as an N self-adjoint matrix. We can see that the three-term recursions (12), (13) correspond to those in the proposition II-C. It is concluded from this fact that the discrete CLN algorithm can be regarded as the Lanczos algorithm with respect to a self-adjoint matrix. The above conclusion suggests that we can extend the discrete CLN method to general discrete systems with symmetric positive definite matrices. It also inferred that the discrete CLN method can be linked to the PVL approximation because both are based on the Lanczos algorithm. In the following section, we propose a new method of MOR that allows the computation of a continued fraction expansion of a transfer function for a given discrete system by extending the discrete CLN algorithm. Thus, any discrete system with symmetric positive definite matrices can be represented by a Cauer circuit because the impedance and admittance of the Cauer circuit are written as continued fraction.

III. Formulation

In this section, we consider a single-input single-output (SISO) linear time-invariant system that satisfies

$$(\mathrm{K}+s\mathrm{N})\boldsymbol{x}=\boldsymbol{b}u(s), \tag{17a}$$
$$y(s)=\boldsymbol{b}^{\mathrm{T}}\boldsymbol{x} \tag{17b}$$

where $\mathrm{K},\mathrm{N}\in\mathbb{R}^{N\times N}$ are symmetric positive definite matrices, $\boldsymbol{b}\in\mathbb{R}^N$ is an arbitrary non-zero vector, $\boldsymbol{x}\in\mathbb{C}^N$, and $s\in\mathbb{C}$. From (17), we obtain

$$\begin{aligned}\mathcal{H}(s)&=\frac{y(s)}{u(s)}\\&=\boldsymbol{b}^{\mathrm{T}}(\mathrm{K}+s\mathrm{N})^{-1}\boldsymbol{b}\\&=\boldsymbol{l}^{\mathrm{T}}(\mathrm{I}-s\mathrm{A})^{-1}\boldsymbol{r}\end{aligned} \tag{18}$$

where $\boldsymbol{l}=\boldsymbol{b}$, $\boldsymbol{r}=\mathrm{K}^{-1}\boldsymbol{b}$, $\mathrm{A}=-\mathrm{K}^{-1}\mathrm{N}$.

A. Computation of orthogonal basis

We propose here Algorithm 3 for a system (17) that is an extension of Algorithm 2. Thus, Algorithm 3 can be applied to not only the FE matrix for quasi-static Maxwell's equation but also to general systems represented by (17).

Vectors $\boldsymbol{u}_n$ and $\boldsymbol{v}_n$ computed from Algorithm 3 are orthogonal with respect to the K and N inner products, respectively. They can be written as

$$(\boldsymbol{u}_i,\boldsymbol{u}_j)_{\mathrm{K}}=\kappa_{2i}\delta_{ij}, \tag{19a}$$
$$(\boldsymbol{v}_i,\boldsymbol{v}_j)_{\mathrm{N}}=\kappa_{2i-1}\delta_{ij} \tag{19b}$$

where δ_{ij} is the Kronecker delta. Since we assume that matrices K, N are the positive definite matrices, the obtained values κ_n are all positive. From this fact, we can conclude that the obtained Cauer circuit is stable and passive.

B. Continued fraction expansion

In this subsection, we show that coefficients κ_n in (19) correspond to the terms of the continued fraction expansion

Algorithm 3 Framework of the proposed algorithm

1: Set $\boldsymbol{u}_0=\boldsymbol{r}=\mathrm{K}^{-1}\boldsymbol{b}$, $\boldsymbol{u}_{-1}=\boldsymbol{0}$, $\boldsymbol{v}_0=\boldsymbol{0}$.
2: Compute κ_0 by (19).
3: **for** n=1 to q **do**
4: Set $\boldsymbol{v}_n=\boldsymbol{v}_{n-1}-\frac{1}{\kappa_{2n-2}}\boldsymbol{u}_{n-1}$.
5: Compute κ_{2n-1} by (19).
6: Set $\boldsymbol{u}_n=\boldsymbol{u}_{n-1}-\frac{1}{\kappa_{2n-1}}\mathrm{A}\boldsymbol{v}_n$.
7: Compute κ_{2n} by (19).
8: **end for**

of a transfer function (18). Let us consider the Taylor series expansion of (18) given by

$$\mathcal{H}(s)=\sum_{i=0}^{\infty}m_i s^i \tag{20}$$

where $m_i=\boldsymbol{l}^{\mathrm{T}}\mathrm{A}^i\boldsymbol{r}$ are referred to as the moments. The moments are computed by the orthogonal vectors obtained from Algorithm 3. From Algorithm 3, we have

$$\begin{aligned}\mathrm{A}\boldsymbol{u}_n=&\kappa_{2n}\kappa_{2n+1}\boldsymbol{u}_{n+1}\\&-\kappa_{2n}(\kappa_{2n+1}+\kappa_{2n-1})\boldsymbol{u}_n+\kappa_{2n}\kappa_{2n-1}\boldsymbol{u}_{n-1}\end{aligned} \tag{21}$$

where $n=0,1,\cdots,q-1$. It can be written in a matrix form as

$$\mathrm{AU}=\mathrm{UT}_q+\kappa_{2q-2}\kappa_{2q-1}\boldsymbol{u}_q\boldsymbol{e}_q^{\mathrm{T}} \tag{22}$$

where $\boldsymbol{e}_q=[0\ 0\ \cdots\ 0\ 1]^{\mathrm{T}}\in\mathbb{R}^q$, $\mathrm{U}=[\boldsymbol{u}_0\ \boldsymbol{u}_1\ \cdots\ \boldsymbol{u}_{q-1}]\in\mathbb{R}^{N\times q}$, and $\mathrm{T}_q\in\mathbb{R}^{q\times q}$ is a tridiagonal matrix defined as

$$\mathrm{T}_q=\begin{bmatrix}-\kappa_0\kappa_1 & \kappa_1\kappa_2 & \cdots & 0\\ \kappa_0\kappa_1 & -\kappa_2(\kappa_1+\kappa_3) & & \\ 0 & \kappa_2\kappa_3 & \ddots & \\ \vdots & \ddots & \ddots & \\ & & & \kappa_{2q-2}\kappa_{2q-3}\\ 0 & & & -\kappa_{2q-2}(\kappa_{2q-3}+\kappa_{2q-1})\end{bmatrix}. \tag{23}$$

Using (19), (22), it can be shown that

$$\mathrm{T}_q^{\mathrm{T}}=\mathrm{D}_e\mathrm{T}_q\mathrm{D}_e^{-1} \tag{24}$$

where $\mathrm{D}_e=\mathrm{U}^{\mathrm{T}}\mathrm{KU}=\mathrm{diag}[\kappa_0\ \kappa_2\ \cdots\ \kappa_{2q-2}]\in\mathbb{R}^{q\times q}$. We can also derive the formulas given by

$$\mathrm{A}^i\boldsymbol{r}=\mathrm{A}^i\boldsymbol{u}_0=\mathrm{A}^i\mathrm{U}\boldsymbol{e}_1=\mathrm{UT}_q^i\boldsymbol{e}_1\quad(0\le i\le q-1), \tag{25a}$$

$$\begin{aligned}\boldsymbol{l}^{\mathrm{T}}\mathrm{A}^i&=\boldsymbol{l}^{\mathrm{T}}\mathrm{K}^{-1}\mathrm{K}\mathrm{A}^i=\boldsymbol{r}^{\mathrm{T}}\mathrm{K}\mathrm{A}^i\\&=-\boldsymbol{u}_0^{\mathrm{T}}(\mathrm{A}^{i-1})^{\mathrm{T}}\mathrm{N}=\boldsymbol{u}_0^{\mathrm{T}}(\mathrm{A}^i)^{\mathrm{T}}\mathrm{K}\\&=\boldsymbol{e}_1^{\mathrm{T}}(\mathrm{A}^i\mathrm{U})^{\mathrm{T}}\mathrm{K}=\boldsymbol{e}_1^{\mathrm{T}}\mathrm{D}_e\mathrm{T}_q^i\mathrm{D}_e^{-1}\mathrm{U}^{\mathrm{T}}\mathrm{K}\\&=\kappa_0\boldsymbol{e}_1^{\mathrm{T}}\mathrm{T}_q^i\mathrm{D}_e^{-1}\mathrm{U}^{\mathrm{T}}\mathrm{K}\quad(0\le i\le q-1)\end{aligned} \tag{25b}$$

where $\boldsymbol{e}_1=[1\ 0\ 0\ \cdots\ 0]^{\mathrm{T}}\in\mathbb{R}^q$. Using (25), moments m_i $(i=0,1,\cdots,2q-2)$ are expressed as

$$\begin{aligned}m_i&=\kappa_0\boldsymbol{e}_1^{\mathrm{T}}\mathrm{T}_q^i\mathrm{D}_e^{-1}\mathrm{U}^{\mathrm{T}}\mathrm{KUT}_q^i\boldsymbol{e}_1\\&=\kappa_0\boldsymbol{e}_1^{\mathrm{T}}\mathrm{T}_q^i\mathrm{D}_e^{-1}\mathrm{D}_e\mathrm{T}_q^i\boldsymbol{e}_1\\&=\kappa_0\boldsymbol{e}_1^{\mathrm{T}}\mathrm{T}_q^i\boldsymbol{e}_1.\end{aligned} \tag{26}$$

Also we have the same result for $i = 2q-1 = q-1+q$ as follows:

$$\begin{aligned} m_{2q-1} &= \kappa_0 \boldsymbol{e}_1^{\mathrm{T}} \mathrm{T}_q^{q-1} \mathrm{D}_e^{-1} \mathrm{U}^{\mathrm{T}} \mathrm{K} (\mathrm{U} \mathrm{T}_q^q \boldsymbol{e}_1 + c\boldsymbol{u}_q) \\ &= \kappa_0 \boldsymbol{e}_1^{\mathrm{T}} \mathrm{T}_q^{2q-1} \boldsymbol{e}_1 + c\kappa_0 \boldsymbol{e}_1^{\mathrm{T}} \mathrm{T}_q^{q-1} \mathrm{D}_e^{-1} \mathrm{U}^{\mathrm{T}} \mathrm{K} \boldsymbol{u}_q \\ &= \kappa_0 \boldsymbol{e}_1^{\mathrm{T}} \mathrm{T}_q^{2q-1} \boldsymbol{e}_1 \end{aligned} \tag{27}$$

where c is a constant. The second term of the second in the third line vanishes because it holds that $(\boldsymbol{u}_q, \boldsymbol{u}_i)_{\mathrm{K}} = 0, i = 0, 1, \cdots, q-1$. Therefore, we have

$$\begin{aligned} \mathcal{H}(s) &\approx \kappa_0 \sum_{i=0}^{2q-1} \boldsymbol{e}_1^{\mathrm{T}} \mathrm{T}_q^i \boldsymbol{e}_1 s^i \\ &= \kappa_0 \boldsymbol{e}_1^{\mathrm{T}} (\mathrm{I} - s\mathrm{T}_q)^{-1} \boldsymbol{e}_1 s^i. \end{aligned} \tag{28}$$

In the PVL approximation, the approximated transfer function (28) is expanded to a partial fraction by the eigenvalue decomposition of T_q[6]. In the proposed method, the transfer function is represented by a continued fraction without eigenvalue decomposition. We can easily show that

$$\mathrm{T}_q = -\mathrm{S}^{\mathrm{T}} \mathrm{D}_o \mathrm{S} \mathrm{D}_e \tag{29}$$

where $\mathrm{D}_o = \mathrm{V}^{\mathrm{T}} \mathrm{N} \mathrm{V} = \mathrm{diag}[\kappa_1 \ \kappa_3 \ \cdots \ \kappa_{2q-1}] \in \mathbb{R}^{q \times q}$, $\mathrm{V} = [\boldsymbol{v}_1 \ \boldsymbol{v}_2 \ \cdots \ \boldsymbol{v}_q] \in \mathbb{R}^{N \times q}$, and $\mathrm{S} \in \mathbb{R}^{q \times q}$ denotes

$$\mathrm{S} = \begin{bmatrix} 1 & -1 & 0 & \cdots & 0 \\ 0 & 1 & -1 & \cdots & 0 \\ 0 & 0 & 1 & \cdots & 0 \\ & \vdots & & \ddots & \\ 0 & 0 & 0 & \cdots & 1 \end{bmatrix}. \tag{30}$$

Substituting T_q in (28) results in

$$\begin{aligned} \mathcal{H}_q(s) &= \kappa_0 \boldsymbol{e}_1^{\mathrm{T}} (\mathrm{I} + s\mathrm{S}^{\mathrm{T}} \mathrm{D}_o \mathrm{S} \mathrm{D}_e)^{-1} \boldsymbol{e}_1 \\ &= \kappa_0 \boldsymbol{e}_1^{\mathrm{T}} \mathrm{D}_e^{-1} (\mathrm{D}_e^{-1} + s\mathrm{S}^{\mathrm{T}} \mathrm{D}_o \mathrm{S})^{-1} \boldsymbol{e}_1 \\ &= \boldsymbol{e}_1^{\mathrm{T}} (\mathrm{D}_e^{-1} + s\mathrm{S}^{\mathrm{T}} \mathrm{D}_o \mathrm{S})^{-1} \boldsymbol{e}. \end{aligned} \tag{31}$$

It is found that (31) is equivalent to the transfer function of the reduced system given by

$$(\mathrm{D}_e^{-1} + s\mathrm{S}^{\mathrm{T}} \mathrm{D}_o \mathrm{S}) \boldsymbol{x} = \boldsymbol{e}_1 V_{in}, \tag{32a}$$

$$I_{out} = \boldsymbol{e}_1^{\mathrm{T}} \boldsymbol{x} = x_0 \tag{32b}$$

where the second term of the left-hand side of (32a) can be written as

$$\mathrm{S}^{\mathrm{T}} \mathrm{D}_o \mathrm{S} = \begin{bmatrix} \kappa_1 & -\kappa_1 & & & \\ -\kappa_1 & \kappa_1 + \kappa_3 & & \ddots & \\ & \ddots & \ddots & & -\kappa_{2q-3} \\ & & & -\kappa_{2q-3} & \kappa_{2q-3} + \kappa_{2q-1} \end{bmatrix}. \tag{33}$$

Now, it is found that the system (32) is equal to the KVL equation of the Cauer circuit that is shown in Fig. 3. Because the transfer function of the system (32) is equal to the admittance of the Cauer circuit, it can be written as

$$\begin{aligned} \mathcal{H}_q(s) &= \frac{I_{out}}{V_{in}} \\ &= \cfrac{1}{\frac{1}{\kappa_0} + \cfrac{1}{\frac{1}{s\kappa_1} + \cfrac{1}{\frac{1}{\kappa_2} + \cfrac{\ddots}{\frac{1}{\kappa_{2q-2}} + \cfrac{1}{\frac{1}{s\kappa_{2q-1}}}}}}} \\ &= \left[0; \tfrac{1}{\kappa_0}, \tfrac{1}{s\kappa_1}, \tfrac{1}{\kappa_2}, \cdots, \tfrac{1}{s\kappa_{2q-1}}\right]. \end{aligned} \tag{34}$$

It is concluded from the above discussion that the continued fraction expansion of the transfer function is directly obtained from the proposed algorithm.

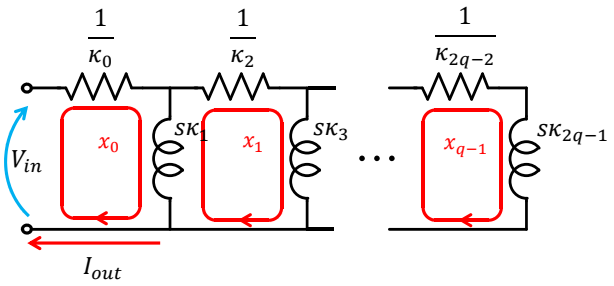

Fig. 3. Circuit representation of the reduced system obtained from the transfer function

IV. Numerical Result

In this section, we consider numerical examples to test the validity of the proposed method.

A. Two-dimensional system

First, we consider a simple system governed by

$$(\mathrm{G} + s\mathrm{C}) \boldsymbol{x} = \boldsymbol{b} u \tag{35a}$$

$$y = \boldsymbol{b}^{\mathrm{T}} \boldsymbol{x} \tag{35b}$$

where u and y are the input and output, respectively, and

$$\mathrm{G} = \begin{bmatrix} 2 & 0 \\ 0 & 1 \end{bmatrix}, \quad \mathrm{C} = \begin{bmatrix} 8 & 2 \\ 2 & 5 \end{bmatrix}, \quad \boldsymbol{b} = \begin{bmatrix} 1 \\ 2 \end{bmatrix}.$$

$\mathrm{A} = -\mathrm{G}^{-1}\mathrm{C}$ is given by

$$\mathrm{A} = \begin{bmatrix} -4 & -1 \\ -2 & -5 \end{bmatrix}. \tag{36}$$

Note that A is not symmetric, whereas G and C are self-adjoint matrices. The transfer function is analytically given by

$$\begin{aligned}\mathcal{H}(s) &= \boldsymbol{b}^{\mathrm{T}}(\mathrm{G}+s\mathrm{C})^{-1}\boldsymbol{b}\\ &= \begin{bmatrix}1 & 2\end{bmatrix}\begin{bmatrix}2+8s & 2s\\ 2s & 1+5s\end{bmatrix}^{-1}\begin{bmatrix}1\\2\end{bmatrix}\\ &= \frac{1}{36s^2+18s+2}\begin{bmatrix}1 & 2\end{bmatrix}\begin{bmatrix}1+5s & -2s\\ -2s & 2+8s\end{bmatrix}\begin{bmatrix}1\\2\end{bmatrix}\\ &= \frac{29s+9}{10s^2+12s+2}\\ &= \left[0; \tfrac{2}{9}, \tfrac{81}{104s}, \tfrac{2704}{225}, \tfrac{25}{936s}\right]. \end{aligned} \tag{37}$$

The continued fraction in the last line is obtained using the Euclidean algorithm. By applying Algorithm 3 to (35), the orthogonal basis and constants κ_n are obtained as follows:

$$\boldsymbol{u}_0 = \mathrm{G}^{-1}\boldsymbol{b} = \begin{bmatrix}\frac{1}{2} & 0\\ 0 & 1\end{bmatrix}\begin{bmatrix}1\\2\end{bmatrix} = \begin{bmatrix}\frac{1}{2}\\2\end{bmatrix}$$

$$\kappa_0 = (\boldsymbol{u}_0, \boldsymbol{u}_0)_{\mathrm{G}} = \begin{bmatrix}\frac{1}{2} & 2\end{bmatrix}\begin{bmatrix}2 & 0\\ 0 & 1\end{bmatrix}\begin{bmatrix}\frac{1}{2}\\2\end{bmatrix} = \frac{9}{2}$$

$$\boldsymbol{v}_1 = -\frac{1}{\kappa_0}\boldsymbol{u}_0 = -\frac{2}{9}\begin{bmatrix}\frac{1}{2}\\2\end{bmatrix} = \begin{bmatrix}-\frac{1}{9}\\-\frac{4}{9}\end{bmatrix}$$

$$\kappa_1 = (\boldsymbol{v}_1, \boldsymbol{v}_1)_{\mathrm{C}} = \begin{bmatrix}-\frac{1}{9} & -\frac{4}{9}\end{bmatrix}\begin{bmatrix}8 & 2\\ 2 & 5\end{bmatrix}\begin{bmatrix}-\frac{1}{9}\\-\frac{4}{9}\end{bmatrix} = \frac{104}{81}$$

$$\boldsymbol{u}_1 = \boldsymbol{u}_0 - \frac{1}{\kappa_1}\mathrm{A}\boldsymbol{v}_1 = \begin{bmatrix}\frac{1}{2}\\2\end{bmatrix} - \frac{104}{81}\begin{bmatrix}-4 & -1\\ -2 & -5\end{bmatrix}\begin{bmatrix}-\frac{1}{9}\\-\frac{4}{9}\end{bmatrix} = \begin{bmatrix}-\frac{5}{26}\\-\frac{5}{52}\end{bmatrix}$$

$$\kappa_2 = (\boldsymbol{u}_1, \boldsymbol{u}_1)_{\mathrm{G}} = \begin{bmatrix}-\frac{5}{26} & -\frac{5}{52}\end{bmatrix}\begin{bmatrix}2 & 0\\ 0 & 1\end{bmatrix}\begin{bmatrix}-\frac{5}{26}\\-\frac{5}{52}\end{bmatrix} = \frac{225}{2704}$$

$$\boldsymbol{v}_2 = \boldsymbol{v}_1 - \frac{1}{\kappa_2}\boldsymbol{u}_1 = \begin{bmatrix}-\frac{1}{9}\\-\frac{4}{9}\end{bmatrix} - \frac{2704}{225}\begin{bmatrix}-\frac{5}{26}\\-\frac{5}{52}\end{bmatrix} = \begin{bmatrix}\frac{11}{5}\\-\frac{8}{5}\end{bmatrix}$$

$$\kappa_3 = (\boldsymbol{v}_2, \boldsymbol{v}_2)_{\mathrm{C}} = \begin{bmatrix}\frac{11}{5} & -\frac{8}{5}\end{bmatrix}\begin{bmatrix}8 & 2\\ 2 & 5\end{bmatrix}\begin{bmatrix}\frac{11}{5}\\-\frac{8}{5}\end{bmatrix} = \frac{936}{25}$$

From this result, we confirm that each term in the continued fraction expansion of the transfer function is obtained by the proposed algorithm.

B. Application to reactor model

1) Reactor model and formulation

As the second numerical example, we consider a magnetic reactor widely used in power electric circuits. For simplicity, the magnetic reactor is assumed to be axisymmetric, as shown Fig.4, whereas the proposed method can be applied to 3D problems in principle. When using a mesh with 166681 elements and 83491 nodes, the FE analysis of the time response of this magnetic reactor excited by a pulse width modulation (PWM) requires approximately 30 h when using Intel(R) Core i7-7700 CPU @ 3.60 GHz, RAM 8.00 GB.

The CLN method is based on the structure of quasi-static Maxwell's equations, whereas the proposed method is formulated starting from the system in (17). When we analyze the magnetic reactor using the $A-\phi$ method, it is found that the FE equations are expressed in the form of (17). Therefore, we choose this model for the numerical example.

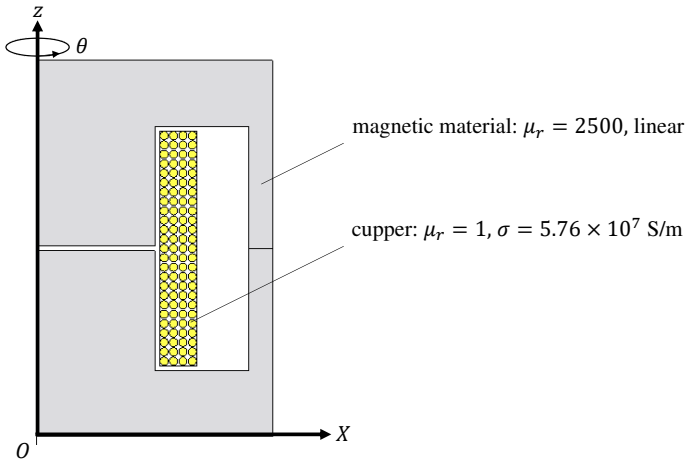

Fig. 4. Axisymmetric reactor

The magnetic reactor is assumed to be composed of a magnetic material with a constant permeability and coil winding. Relative permeability μ_r of the magnetic material is set as 2500. Radius of the wire a is 1.75×10^{-4} m and its conductivity σ is 5.76×10^{7} S/m. The governing equations are given by

$$\nabla\times(\nu\nabla\times\boldsymbol{A}) + \mathrm{j}\omega\sigma(\boldsymbol{A}+\nabla\phi) = \boldsymbol{J}_{ext}, \tag{38a}$$

$$\mathrm{j}\omega\nabla\cdot(\boldsymbol{A}+\nabla\phi) = 0 \tag{38b}$$

where ν, ω, and $\boldsymbol{J}_{ext}$ are the reciprocal of the magnetic permeability, angular frequency, and current density of the external current density, respectively. The equations are considered in the (r,z,θ) cylindrical coordinate system. Equation (38b) is the current constraint condition over the wire cross-sections. Note that potential ϕ, which is constant in each wire cross-section, can take different values $\phi_k : k=1,2,\cdots,m$, where m is the number of turns. The boundary condition is given by

$$\mu\boldsymbol{H}\cdot\boldsymbol{n} = 0 \quad on\ \Gamma_n. \tag{39}$$

In the FE formulation, the unknowns are discretized into

$$\boldsymbol{A} = \sum_{i=0}^{n} A_i N_i \boldsymbol{e}_\theta, \tag{40a}$$

$$\phi = N_\theta \Delta V_k = \frac{\theta}{2\pi}\Delta V_k \quad in\ S_k\ (k=1,2,\cdots,m) \tag{40b}$$

where N_i is the node interpolation function defined in the elements, $\boldsymbol{e}_\theta$ is the unit vector in θ-direction, S_k is the cross-section of the k-th wire, N_θ is the interpolation function to represent the voltage drop along the wires, and ΔV_k is the voltage drop from $\theta=0$ to 2π. Thus, the number of unknowns are $n+m$, where n is the number of nodes.

The governing equations are discretized into a linear algebraic equation by FEM as follows:

$$\left(\begin{bmatrix}\mathrm{K} & \mathrm{O}_{nm}\\ \mathrm{O}_{mn} & \mathrm{O}_{nn}\end{bmatrix} + s\begin{bmatrix}\mathrm{N} & \mathrm{D}\\ \mathrm{D}^{\mathrm{T}} & \mathrm{E}\end{bmatrix}\right)\begin{bmatrix}\boldsymbol{a}\\ \Delta\boldsymbol{V}\end{bmatrix} = \begin{bmatrix}\boldsymbol{b}\\ \boldsymbol{0}\end{bmatrix} i \tag{41}$$

where $\mathrm{K},\mathrm{N}\in\mathbb{R}^{n\times n}$, $\mathrm{D}\in\mathbb{R}^{n\times m}$, $\mathrm{E}\in\mathbb{R}^{m\times m}$, and $\boldsymbol{b}\in\mathbb{R}^n$

are given by

$$\mathrm{K}_{ij} = \int_\Omega \nabla \times N_i \boldsymbol{e}_\theta \cdot \nu \nabla \times N_j \boldsymbol{e}_\theta d\Omega, \tag{42a}$$

$$\mathrm{N}_{ij} = \int_\Omega \sigma N_i \boldsymbol{e}_i \cdot N_j \boldsymbol{e}_\theta d\Omega, \tag{42b}$$

$$\mathrm{D}_{ik} = \int_{S_k} \sigma N_i \boldsymbol{e}_\theta \cdot \nabla N_\theta d\Omega, \tag{42c}$$

$$\mathrm{E}_{kk} = \int_{S_k} \sigma \nabla N_k \cdot \nabla N_k d\Omega, \tag{42d}$$

$$b_i = \int_\Omega N_i \boldsymbol{e}_\theta \cdot \boldsymbol{j} d\Omega \tag{42e}$$

where $\boldsymbol{j}$ is the current density when there is a unit current flow in the wire and i is the input current. The voltage between the wire terminals can be written as

$$\begin{aligned} v &= s \int_\Omega \boldsymbol{A} \cdot \boldsymbol{j} d\Omega + R_{DC} i = s \boldsymbol{b}^{\mathrm{T}} \boldsymbol{a} + R_{DC} i \\ &= s \begin{bmatrix} \boldsymbol{b}^{\mathrm{T}} & \boldsymbol{0} \end{bmatrix} \begin{bmatrix} \boldsymbol{a} \\ \Delta \boldsymbol{V} \end{bmatrix} + R_{DC} i \end{aligned} \tag{43}$$

where R_{DC} represents the DC resistance of the winding. Thus, the transfer function of this system can be expressed as

$$\begin{aligned} \mathcal{H}(s) &= \frac{v}{i} \\ &= s \begin{bmatrix} \boldsymbol{b}^{\mathrm{T}} & \boldsymbol{0} \end{bmatrix} \left(\begin{bmatrix} \mathrm{K} & \mathrm{O}_{nm} \\ \mathrm{O}_{mn} & \mathrm{O}_{nn} \end{bmatrix} + s \begin{bmatrix} \mathrm{N} & \mathrm{D} \\ \mathrm{D}^{\mathrm{T}} & \mathrm{E} \end{bmatrix} \right)^{-1} \begin{bmatrix} \boldsymbol{a} \\ \Delta \boldsymbol{V} \end{bmatrix} \\ &\quad + R_{DC}. \end{aligned} \tag{44}$$

The transfer function cannot be computed by the proposed method because the first matrix is not invertible. To avoid this problem, voltage drops $\Delta \boldsymbol{V}$ are eliminated from (41). Inserting $\Delta \boldsymbol{V} = -\mathrm{E}^{-1}\mathrm{D}^{\mathrm{T}} \boldsymbol{a}$ in (41a) results in

$$\Big(\mathrm{K} + s(\mathrm{N} - \mathrm{D}\mathrm{E}^{-1}\mathrm{D}^{\mathrm{T}}) \Big) \boldsymbol{a} = \boldsymbol{b} i. \tag{45}$$

The transfer function is now re-written as

$$\mathcal{H}(s) = \frac{v}{i} = s \boldsymbol{b}^{\mathrm{T}} \Big(\mathrm{K} + s(\mathrm{N} - \mathrm{D}\mathrm{E}^{-1}\mathrm{D}^{\mathrm{T}}) \Big)^{-1} \boldsymbol{b} + R_{DC}. \tag{46}$$

The proposed method can be applied to this transfer function because K is invertible. The equivalent Cauer circuit of the transfer function is shown in Fig. 5. Note that we do not have to compute $\mathrm{D}\mathrm{E}^{-1}\mathrm{D}^{\mathrm{T}}$, which is a dense matrix, because only the matrix-vector product is required in the proposed method.

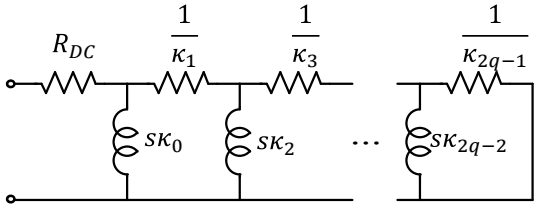

Fig. 5. Cauer circuit obtained from the FE equation of the axisymmetric reactor

2) Numerical result

Circuit constants κ_n of the Cauer circuit obtained by the proposed method are summarized in Table. I. The frequency characteristics of the reactor are computed by FEM and the obtained equivalent circuit, as shown in Fig.6. To evaluate the dependence on the number of stages, stage number q is increased from 2 to 4. The left figure is the characteristic of the real part of the impedance, which represents the AC resistance, whereas the right is the imaginary part, which represents the stored magnetic energy. We can see that the results obtained by using the equivalent circuit are in good agreement with those yielded by FEM, particularly when $q \geq 4$.

It takes only 49 s to construct a five-stage Cauer circuit that is obtained by truncating Algorithm 3 at $q = 4$. While the conventional FEM needs solving the FE equation numerous times to obtain the time response, we can rapidly obtain the time response to solve the circuit equation of the obtained Cauer circuit because the dimension of the circuit equation is much smaller than that of the FE equation.

TABLE I
CIRCUIT CONSTANTS OBTAINED BY THE PROPOSED METHOD

n	κ_{2n}	κ_{2n+1}
0	5.02×10^{-3}	2.27×10^{-6}
1	1.97×10^{-1}	1.02×10^{-7}
2	1.82×10^{0}	8.43×10^{-8}
3	2.01×10^{0}	3.04×10^{-8}
4	7.05×10^{0}	1.84×10^{-4}

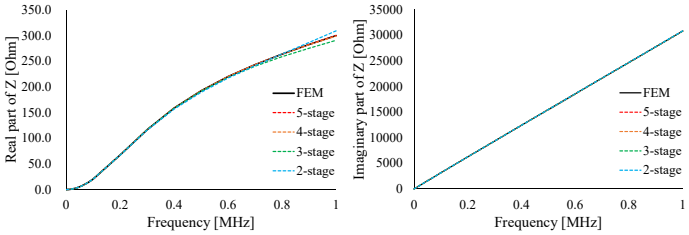

Fig. 6. Frequency characteristics of the impedance

Then, we performed the time domain analysis of the obtained Cauer circuit excited by a 200 kHz PWM, which is shown in Fig.7. In the time domain analysis, the stage number is fixed to $q = 4$. The waveforms of the current and Joule losses are plotted in Figs.8 and 9, respectively. The results obtained from FEM and the zero-th order circuit are also plotted in the figures. The impedance of the zero-th order circuit is $s\kappa_0 + R_{DC}$, in which the eddy currents are not considered. We can see that the current waveforms cannot be distinguished from each other, whereas the Joule losses obtained by zero-th order circuit is different from the others because of the eddy current effects. We can also see that the waveform of the Joule losses obtained by the Cauer circuit is in good agreement with that obtained by FEM. We conclude from these results that the eddy current effects are accurately evaluated by the Cauer circuit.

Note that it takes approximately 2.2 s to obtain the time response by the Cauer circuit, whereas it takes approximately 30 h to do so by FEM. In addition, the Cauer circuit can

simulate eddy current losses comparable to those obtained by FEM.

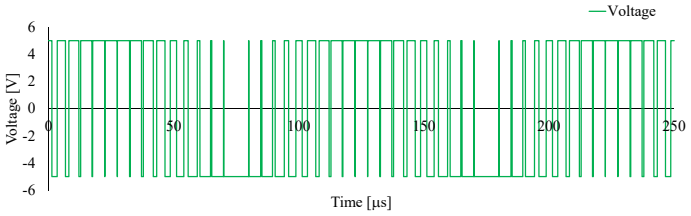

Fig. 7. Waveform of the PWM excitation

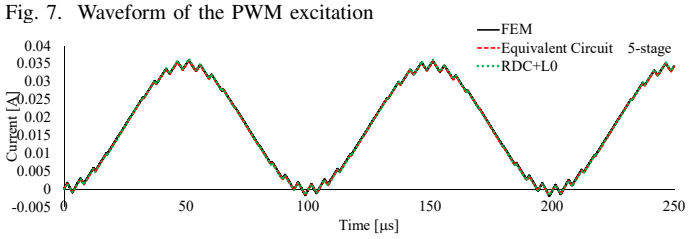

Fig. 8. Waveform of the current

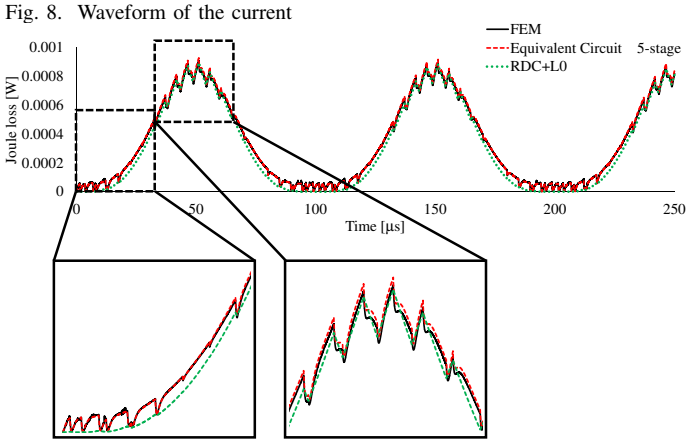

Fig. 9. Waveform of the Joule losses

V. Conclusion

In this paper, we have introduced a new algorithm to generate a reduced model of a linear time-invariant system with symmetric positive definite matrices. The reduced model is represented by a Cauer circuit because the transfer function of the original system is approximated to a rational function that has the form of a continued fraction. The algorithm can be seen as an extension of the discrete CLN algorithm because its application is not limited to systems governed by quasi-static Maxwell's equations. The validity of the proposed method is shown considering a simple mathematical problem. Moreover, the eddy current effects in a magnetic reactor are shown to be accurately evaluated by the resultant Cauer circuit. We have restricted ourselves to problems with constant material property in this paper. However, we expect that the proposed method can also be applied to parametrized problems in which, e.g., permeability is a function of frequency.

In the future work, we will discuss the theoretical reason behind being able to obtain the continued fraction representation of a given transfer function. We will reveal the relation between the proposed method and orthogonal polynomials, and we will also extend the proposed method to a more general linear time-invariant system.

Acknowledgement

This work was supported by JSPS KAKENHI Grant Number JP19J20541.

References

[1] J. Biela, M. Schweizer, S. Waffler, and J. W. Kolar, "Sic versus si-evaluation of potentials for performance improvement of inverter and dc-dc converter systems by sic power semiconductors," *IEEE Transactions on Industrial Electronics*, vol. 58, no. 7, pp. 2872–2882, July 2011.

[2] G. Berkooz, P. Holmes, and J. L. Lumley, "The proper orthogonal decomposition in the analysis of turbulent flows," *Annual Review of Fluid Mechanics*, vol. 25, no. 1, pp. 539–575, 1993.

[3] A. Chatterjee, "An introduction to the proper orthogonal decomposition," *Current Science*, vol. 78, no. 7, pp. 808–817, 2000.

[4] T. Henneron and S. Clénet, "Model order reduction of non-linear magnetostatic problems based on pod and dei methods," *IEEE Transactions on Magnetics*, vol. 50, no. 2, pp. 33–36, Feb 2014.

[5] T. Shimotani, Y. Sato, and H. Igarashi, "Equivalent-circuit generation from finite-element solution using proper orthogonal decomposition," *IEEE Transactions on Magnetics*, vol. 52, no. 3, pp. 1–4, March 2016.

[6] P. Feldmann and R. W. Freund, "Efficient linear circuit analysis by pade approximation via the lanczos process," *IEEE Transactions on Computer-Aided Design of Integrated Circuits and Systems*, vol. 14, no. 5, pp. 639–649, May 1995.

[7] R. W. Freund, "Krylov-subspace methods for reduced-order modeling in circuit simulation," *Journal of Computational and Applied Mathematics*, vol. 123, no. 1, pp. 395 – 421, 2000, numerical Analysis 2000. Vol. III: Linear Algebra. [Online]. Available: http://www.sciencedirect.com/science/article/pii/S0377042700003964

[8] Z. Bai, "Krylov subspace techniques for reduced-order modeling of large-scale dynamical systems," *Applied Numerical Mathematics*, vol. 43, no. 1, pp. 9 – 44, 2002, 19th Dundee Biennial Conference on Numerical Analysis. [Online]. Available: http://www.sciencedirect.com/science/article/pii/S0168927402001162

[9] Y. Sato and H. Igarashi, "Generation of equivalent circuit from finite-element model using model order reduction," *IEEE Transactions on Magnetics*, vol. 52, no. 3, pp. 1–4, March 2016.

[10] Y. Sato, T. Shimotani, and H. Igarashi, "Synthesis of cauer-equivalent circuit based on model order reduction considering nonlinear magnetic property," *IEEE Transactions on Magnetics*, vol. 53, no. 6, pp. 1–4, June 2017.

[11] A. Kameari, H. Ebrahimi, K. Sugahara, Y. Shindo, and T. Matsuo, "Cauer ladder network representation of eddy-current fields for model order reduction using finite-element method," *IEEE Transactions on Magnetics*, vol. 54, no. 3, pp. 1–4, March 2018.

[12] Y. Shindo, T. Miyazaki, and T. Matsuo, "Cauer circuit representation of the homogenized eddy-current field based on the legendre expansion for a magnetic sheet," *IEEE Transactions on Magnetics*, vol. 52, no. 3, pp. 1–4, March 2016.

[13] C. Lanczos, "Solution of systems of linear equations by minimized iterations," *J. Res. Natl. Bur. Stand*, vol. 49, pp. 33–53, 1952.

[14] M. R. Hestenes and E. Stiefel, "Methods of conjugate gradients for solving linear systems," *Journal of Research of the National Bureau of Standards*, vol. 49, pp. 409–436, 1952.

Shingo Hiruma received the B.E. and M.E. degrees from Hokkaido University, Sapporo, Japan, in 2017 and 2019. He is currently a Ph.D. student in Hokkaido University. His research interest is the computational electromagnetism using model order reduction technique.

Hajime Igarashi received the B.E. and M.E. degrees in electrical engineering from Hokkaido University, Sapporo, Japan, in 1982 and 1984, respectively, and the Ph.D. degree in engineering from Hokkaido University in 1992. He has been a professor at the Graduate School of Information Science and Technology, Hokkaido University, since 2004. His research area is computational electromagnetism, design optimization and energy harvesting. He is a member of IEEE, IEICE, International COMPUMAG society, JSST, JASCOME and JSAEM. He was awarded prize of outstanding technical paper by IEEJ 2016.